Influence of coherent population trapping on Raman scattering

Pooja Singh,[1,2] Anil K. Patnaik,[3,4] Sukesh Roy,[3] James R. Gord,[5] and Yuri V. Rostovtsev[1]
[1]*Center for Nonlinear Sciences and Department of Physics, University of North Texas, Denton, Texas 76203, USA*
[2]*Division of Sciences and Mathematics, Louisiana State University at Eunice, Eunice, Louisiana 70535, USA*
[3]*Spectral Energies LLC, 5100 Springfield Street, Suite 301, Dayton, Ohio 45431,USA*
[4]*Department of Physics, Wright State University, Dayton, Ohio 45435, USA*
[5]*Air Force Research Laboratory, Aerospace Systems Directorate, Wright-Patterson Air Force Base, Ohio 45433, USA*

(Received 15 November 2018; published 8 August 2019)

We have considered the Raman scattering in molecular media. Applying two laser fields in a two-photon resonance with vibrational transition, we have studied the role of rotational levels for excitation of vibrational coherence. It is shown that the molecular vibrational coherence strongly depends on the effect of coherent population trapping for rotational levels. The obtained results are important for applications of Raman spectroscopy to molecular detection in engineering, chemical, and biological applications.

DOI: 10.1103/PhysRevA.100.023808

I. INTRODUCTION

Raman spectroscopy [1–3] is one among many powerful techniques that has been widely used in engineering, chemical, and biological applications. Raman spectroscopy is based on a two-photon optical resonance with vibrational molecular levels (see Fig. 1) when two optical pulses excite the molecular vibrational coherence. In an effort to optimize Raman spectroscopy, techniques have been developed that introduce modified optical pulses and models. Applying the femtosecond adaptive technique allows researchers to excite maximal vibrational coherence to improve the sensitivity of coherent Raman spectroscopy and to perform real-time identification of bacterial spores and biomolecules [4–8]. The femtosecond-laser-based coherent anti-Stokes Raman spectroscopy (CARS) has been used extensively in time-resolved nonlinear spectroscopy research in recent years [9]. It is used in several fields of study, such as identifying molecules in chemistry, measuring temperature in solid-state physics, and noninvasive monitoring of muscle tissue, among other things.

It is the quantum coherent effects that have strong influence on the Raman scattering. Quantum coherence effects, such as coherent population trapping (CPT) [10] and electromagnetically induced transparency (EIT) [11–14], have been the focus of broad research activity for the past decades, as they drastically change optical properties of media. For example, for EIT in continuous-wave(CW) regimes [12–16], absorption practically vanishes.

The medium with excited quantum coherence [11] shows ultradispersive properties [17] and has several orders of magnitude higher spectral dispersion than natural materials [18]. The corresponding steep dispersion results in the ultraslow or ultrafast propagation of light pulses [19–23], which can be used for drastic modification of the phase-matching conditions for Brillouin scattering [24] and four-wave mixing [25]. It has been shown that the optical 0π pulses [26] under the condition of EIT [27,28] are very sensitive to resonant interaction and have advantages for use in Raman spectroscopy.

Recently, the saturation of vibrational Raman coherence and coherent anti-Stokes Raman scattering (CARS) using femtosecond optical pulses has been investigated theoretically [29]. It was demonstrated that the vibrational coherence and also the vibrational CARS with femtosecond excitation display saturation-like behavior once the rotational coherence is saturated. A generalized formulation is developed for determining the saturation thresholds for optical processes excited by ultrafast pulses based on the pulse area of the excitation pulse [30] and for different pulse shapes [31]. The condition was derived for the saturation threshold of a probe pulse in an ultrafast electronic-resonance-enhanced (ERE) coherent anti-Stokes Raman spectroscopy (CARS) configuration [32]. Further, femtosecond fully resonant electronically enhanced CARS (FREE-CARS) has been demonstrated with orders of magnitude enhancement of the CARS signal, where all three input pump, Stokes, and probe pulses are resonant to electronic states of the molecules [33,34].

In this paper, we study excitation of the molecular coherence in a Λ-type molecular media (see Fig. 2). In order to analyze the interaction and gain new insights into a rotational-vibrational system, we restrict ourselves to a simplistic model of a single rotational split of a ground level.

Thus, we consider a four-level molecular medium interacting with the probe and coupling fields (see the Appendix for more details of the simplified system). We have considered the three- and four-level molecules [Figs. 2(a)–2(c)]. The dressed-state basis approach is employed, which provides deep physical insights showing interaction of "bright" and "dark" states with radiation. For the four-level model, we find two sets of the bright and dark states that show the important role of coherent population trapping between split ground states on Raman scattering in such molecular systems. The level structure of the model is common for the molecular media, where the split ground states can be viewed as rotational levels in addition to the vibrational levels with much higher frequency. We demonstrate the importance of formation of dark states between rotational levels on Raman and stimulated

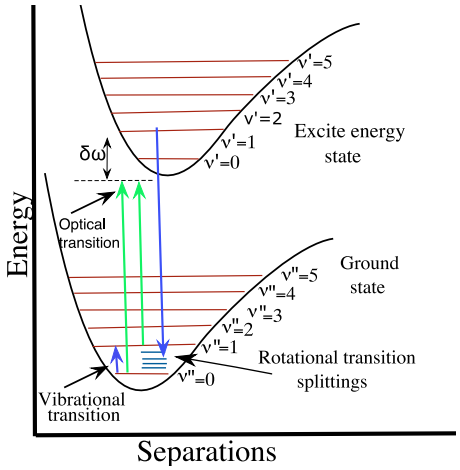

FIG. 1. Molecular levels: ground and excited electronic states, vibrational and rotational levels.

Raman scattering. We consider the propagation effects for the case when the vibrational-rotational coherence is induced. In particular, we consider a gas of three- and four-level atoms or molecules in the presence of two coherent optical pulses.

The paper is organized as follows. In Sec. II, we describe the theoretical model. In Sec. III, we describe the coherent population trapping and its role for the excitation of the vibrational coherence, and we have shown that the rotational levels strongly influence the population transfer as well as the excitation of the vibrational coherence. Section IV extends the discussion to propagation of optical fields in both three- and four- level systems.

Finally, Sec. V presents our discussion and conclusions.

II. MODEL

To describe the interaction of the molecules with optical fields, we employ molecular models that include three- and four-level quantum systems shown in Fig. 2. First, let us consider a Λ-type atomic medium. A strong field of frequency ω_2 is the coupling field and a field of frequency ω_1 is the probe

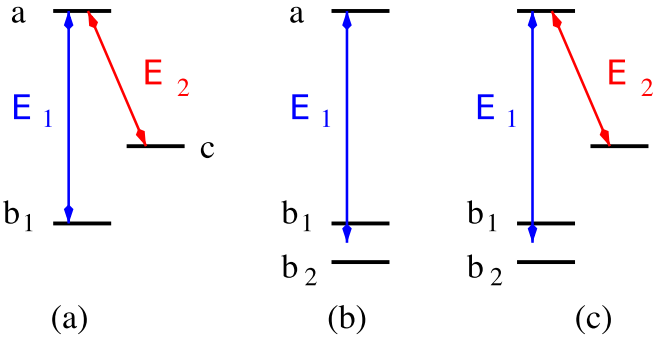

FIG. 2. (a) Energy-level scheme of the three-level Λ-type atoms or molecules. (b) The three-level Λ-type system with two close levels similar to molecular rotational levels (see Fig. 1). (c) A simple four-level model that takes into account the vibrational and rotational molecular levels.

field. The probe and coupling fields can be represented as

$$E_{1,2} = E^0_{1,2} \exp[ik_{1,2}z - i\omega_{1,2}t], \tag{1}$$

where $E^0_{1,2}$ is the amplitudes of fields at $z = 0$. The interaction Hamiltonian in the rotating-wave approximation can be written as

$$H = \hbar[\Omega_1^* e^{i\Delta_1 t}|b\rangle\langle a| + \Omega_2^* e^{i\Delta_2 t}|c\rangle\langle a| + \text{adj.}] \tag{2}$$

where $|b\rangle\langle a|$, and $|c\rangle\langle a|$ are the atomic projection operators, $\Omega_1 = \wp_{ab}E_1/\hbar$ and $\Omega_2 = \wp_{ac}E_2/\hbar$ are the probe and coupling Rabi frequencies, $\Delta_1 = \omega_{ab} - \omega_1$ and $\Delta_2 = \omega_{ac} - \omega_2$ are the detunings for probe and coupling laser beams, and $\wp_{ab}$ and $\wp_{ac}$ are the dipole momenta of the corresponding transitions. Here, ω_{ab} and ω_{ac} are the angular frequency of $|a\rangle \to |b\rangle$ and $|a\rangle \to |c\rangle$ transitions. The coupling field is resonant with the $|a\rangle \to |c\rangle$ transition ($\Delta_2 = 0$).

We consider various relation with the duration of the laser pulses and relaxation times. For the case when the laser pulses are shorter than the relaxation times, we are going to use the state vector approach. The molecular system in Hamiltonian in Eq. (2) is described by the state vector

$$|\psi\rangle = a|a\rangle + b|b\rangle + c|c\rangle, \tag{3}$$

where, a, b, and c are the probability amplitudes of the molecular states $|a\rangle$, $|b\rangle$, and $|c\rangle$, respectively. The Schrödinger equation for the state vectors is given by

$$i\hbar\frac{\partial}{\partial t}|\psi\rangle = \hat{H}|\psi\rangle. \tag{4}$$

To take into account the relaxation processes, we employ the density matrix approach and the equations are given by

$$\frac{\partial\rho}{\partial t} = \frac{i}{\hbar}[\rho, H] - \frac{1}{2}(\Gamma\rho + \rho\Gamma), \tag{5}$$

where Γ is the matrix of relaxation rates for all components of the density matrix ρ. The steady-state evolution of optical fields is determined by the propagation equations

$$\frac{\partial\Omega_1}{\partial z} = -i\eta_1\rho_{ab}, \quad \frac{\partial\Omega_2}{\partial z} = i\eta_2\rho_{ca}, \tag{6}$$

where $\eta_{1,2} = \frac{3\lambda^2_{1,2}N}{8\pi}\gamma_{1,2}$, $\gamma_{1,2}$ are the spontaneous emission relaxation rates for corresponding transitions, $\Gamma_{ca} = \gamma_{ca} - i(\omega_{ac} - \omega_2)$, $\Gamma_{cb} = \gamma_{cb} + i(\omega_{cb} - \omega_1 + \omega_2)$, and $\Gamma_{ab} = \gamma_{ab} + i(\omega_{ab} - \omega_1)$. The Doppler broadening is important to take into account by averaging the polarizations ρ_{ab} and ρ_{ca} over velocity distribution [35].

Similarly, we consider a four-level molecular medium interacting with the probe and coupling fields. For angular frequencies ω_{ab_1} and ω_{ab_2} corresponding to the allowed transitions $|a\rangle \to |b_1\rangle$ and $|a\rangle \to |b_2\rangle$, the interaction Hamiltonian in the rotating-wave approximation can be written as

$$H = \hbar[\Omega_{11}^* e^{i\Delta_{11}t}|b_1\rangle\langle a| + \Omega_{12}^* e^{i\Delta_{12}t}|b_2\rangle\langle a| + \Omega_2^* e^{i\Delta_2 t}|c\rangle\langle a| + \text{adj.}]. \tag{7}$$

Here, $\Omega_{11} = \wp_{ab_1}E_1/\hbar$ and $\Omega_{12} = \wp_{ab_2}E_1/\hbar$ are the coupling Rabi frequencies, $\Delta_{11} = \omega_{ab_1} - \omega_1$ and $\Delta_{12} = \omega_{ab_2} - \omega_1$ are the detunings for probe laser beam, and $\wp_{ab_1}$ and $\wp_{ab_2}$ are the corresponding dipole momenta of the transitions. The state

vector for the four-level system is written as

$$|\psi\rangle = a|a\rangle + b_1|b_1\rangle + b_2|b_2\rangle + c|c\rangle. \quad (8)$$

III. COHERENT POPULATION TRAPPING OF ROTATIONAL AND VIBRATIONAL LEVELS

First, let us consider the molecular system shown in Fig. 2(a). The state vector is given by Eq. (3) and a, b, and c coefficients can be found from the set of equations

$$\dot{a} = -i\Omega_1 b - i\Omega_2 c, \quad (9)$$

$$\dot{b} = -i\Omega_1 a, \quad (10)$$

$$\dot{c} = -i\Omega_2 a. \quad (11)$$

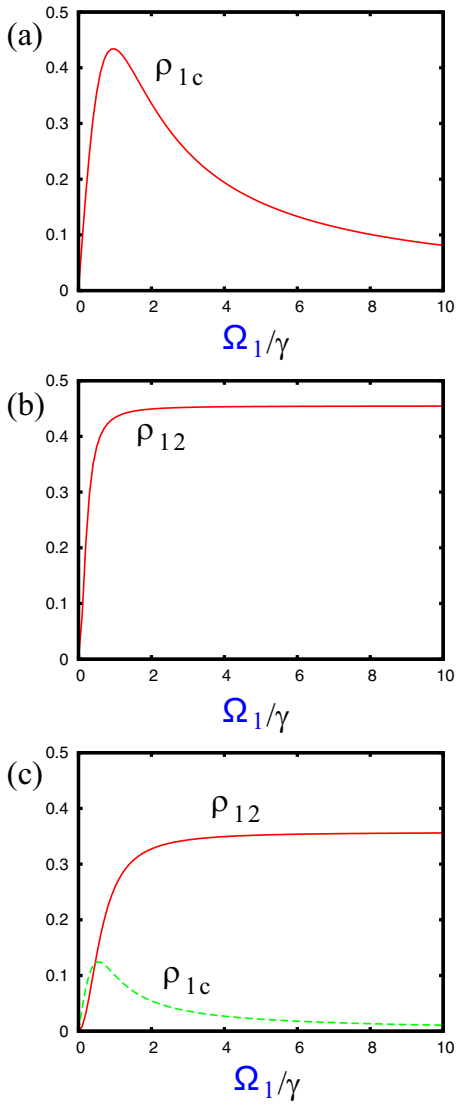

FIG. 3. The bare state basis (a) and the dark-bright state basis (b) for three-level system. For two fields and three-level system, we have one bright state and one dark state. The bare state basis (c) and the dark-bright state basis (d) for the four-level system are shown. The situations for two fields and the four-level system are different; we have one bright state and now we have the whole plane of dark states that are linear combinations of the dark states $|D_v\rangle$ and $|D_j\rangle$ given by Eqs. (25) and (26).

It is instructive to introduce the so-called "dark" and "bright" states [11]

$$|B\rangle = \frac{\Omega_1|b\rangle + \Omega_2|c\rangle}{\Omega_e}, \quad |D\rangle = \frac{\Omega_2|b\rangle - \Omega_1|c\rangle}{\Omega_e}, \quad (12)$$

where $\Omega_e = \sqrt{\Omega_1^2 + \Omega_2^2}$ is the effective Rabi frequency. The Eqs. (9)–(11) can be re-written as

$$\dot{a} = -i\Omega_e B, \quad (13)$$

$$\dot{B} = -i\Omega_e a + gD, \quad (14)$$

$$\dot{D} = -gB, \quad (15)$$

where

$$g = \frac{\dot{\Omega}_1\Omega_2 - \Omega_1\dot{\Omega}_2}{\Omega_1^2 + \Omega_2^2} = \dot{\Theta}, \quad (16)$$

and $\Theta = \arctan\left(\frac{\Omega_1}{\Omega_2}\right)$. Note that g describes the coupling between the "bright" and "dark" states. Although, we should point out that for the adiabatic pulses, $g \simeq 0$, the excited level $a \simeq 0$ and thus the bright state $B \simeq 0$ are not excited. The eigenvalues for Λ scheme are given by

$$\lambda_D = 0, \quad \lambda_\pm = \pm\sqrt{\Omega_1^2 + \Omega_2^2}. \quad (17)$$

In the presence of rotational splittings, corresponding to vibrational levels involved in the three-level energy model, new coherent optical interactions appear. The results of these interfering levels can, however, produce strong variations in excitation of vibrational coherence. For a resulting four-level molecular system shown in Fig. 2(c), the state vector is given by Eq. (A5) and a, b_1, b_2, and c coefficients can be found from the set of equations

$$\dot{a} = -i\Omega_{11} b_1 - i\Omega_{12} b_2 - i\Omega_2 c, \quad (18)$$

$$\dot{b}_1 = -i\Omega_{11} a, \quad (19)$$

$$\dot{b}_2 = -i\Omega_{12} a, \quad (20)$$

$$\dot{c} = -i\Omega_2 a. \quad (21)$$

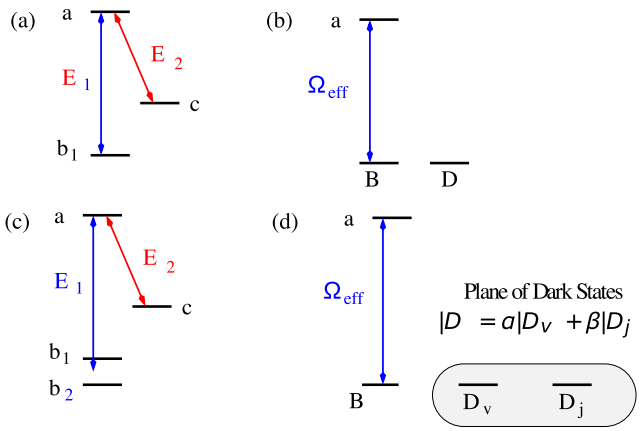

FIG. 4. (a) Excitation of vibrational coherence of molecules shown in Fig. 2(a) ($\Omega_2/\gamma = 1$). (b) Excitation of rotational coherence of molecules shown in Fig. 2(b). (c) Excitation of rotational coherence prevents excitation of vibrational coherence of molecules shown in Fig. 2(c).

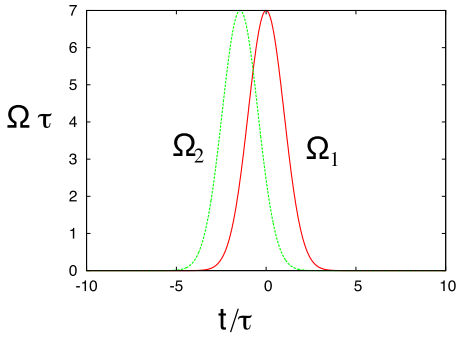

FIG. 5. Gaussian optical pulses $\Omega_1(t)$ and $\Omega_2(t)$ given by Eqs. (27) and (28) to perform the stimulated adiabatic passage to transfer population between molecular vibrational levels as function of time in units of τ. The amplitudes are $\Omega_{01} = 7\tau^{-1}$ and $\Omega_{02} = 7\tau^{-1}$.

Now, the effective Rabi frequency for the system is

$$\Omega_{\pm} = \sqrt{\Omega_{11}^2 + \Omega_{12}^2 + \Omega_2^2}. \tag{22}$$

The eigenvalues for the four-level scheme are

$$\lambda_{1,2} = 0, \quad \lambda_{\pm} = \pm\sqrt{\Omega_{11}^2 + \Omega_{12}^2 + \Omega_2^2}, \tag{23}$$

and the bright states are defined as

$$|B_{\pm}\rangle = \frac{\Omega_{\pm}|a\rangle + \Omega_2|b_1\rangle + \Omega_{12}|c\rangle}{\Omega_e}. \tag{24}$$

It is essential to note here that we have two "dark" states that correspond to the "zero" eigenvalues. One is related to the trapped state between rotational levels and another corresponds to the trapped state between vibrational levels. These dark states are given by

$$|D_j\rangle = \frac{\Omega_{11}|b_1\rangle - \Omega_{12}|b_2\rangle}{\sqrt{\Omega_{11}^2 + \Omega_{12}^2}} \tag{25}$$

and

$$|D_v\rangle = \frac{\Omega_2|b_1\rangle - \Omega_{11}|c\rangle}{\sqrt{\Omega_{11}^2 + \Omega_2^2}}. \tag{26}$$

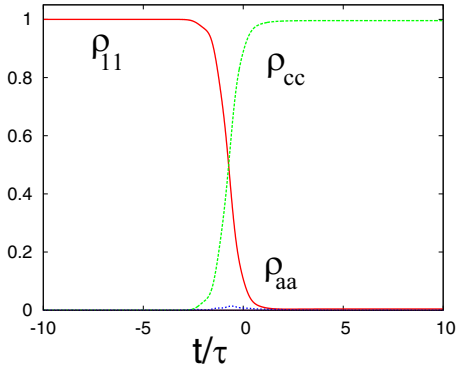

FIG. 6. Population transfer achieved with the optical pulses shown in Fig. 5 for the case of the three-level Λ system [shown in Fig. 2(a)]. ρ_{11} corresponds to population of level b_1.

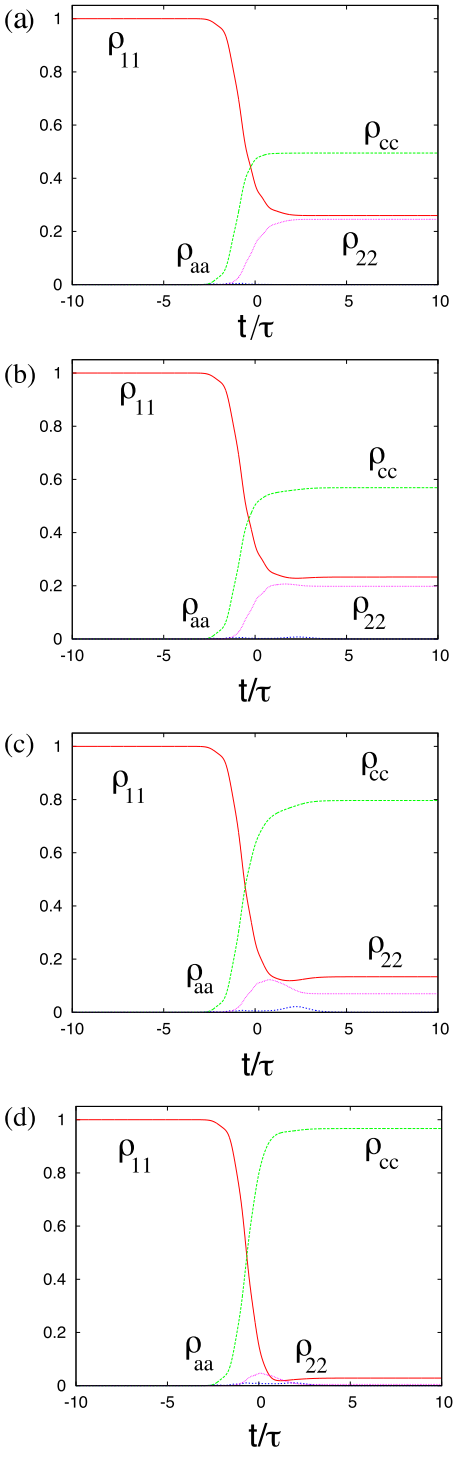

FIG. 7. Adiabatic passage population transfer achieved with STIRAP pulses in four-level atoms with different ratios of the rotational splitting to the Rabi frequency: (a) $\Delta = 0\Omega_{120}$, (b) $\Delta = 0.5\Omega_{120}$, (c) $\Delta = 1\Omega_{120}$, and (d) $\Delta = 2\Omega_{120}$. ρ_{11} and ρ_{22} corresponds to populations of levels b_1 and b_2 respectively.

Let us also note here that any linear combinations of the dark state above are also the dark state, namely the state $|D\rangle = \alpha|D_j\rangle + \beta|D_v\rangle$ for arbitrary numbers α and β is the dark state too, the state that is not coupled with excited state $|a\rangle$ by the laser fields. Figures 3(a) and 3(b) show a three-level system

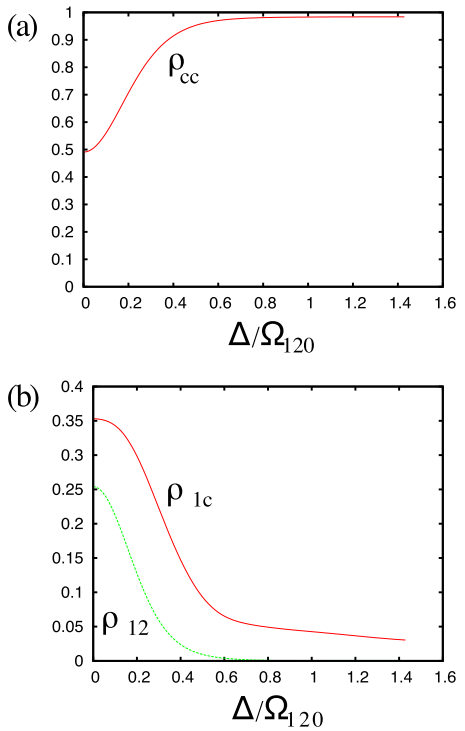

FIG. 8. (a) Population transfer achieved with the optical pulses shown in Fig. 5 for the case of the four-level Λ system [shown in Fig. 2(c)] as a function of Δ/Ω_{120}. (b) The vibrational (ρ_{1c}) and rotational (ρ_{120}) coherences are excited by the pulses.

bare state basis and the corresponding dark- bright state basis with one bright and one dark state. Figures 3(c) and 3(d) show the bare state basis and a dark-bright state basis for the four-level system correspondingly. The situation with the four-level system and two applied fields is different with the possibility of more than one dark state. We have one bright state and a whole plane of dark states that are linear combinations of the dark states $|D_v\rangle$ and $|D_j\rangle$ given by Eqs. (25) and (26).

Usually, with a weak laser field, the three-level atom is a good approximation, but to achieve higher detection sensitivity, a stronger laser field is needed. This, however, has its limitations, because once the Rabi frequency becomes comparable with the rotational frequency, the coherent population trapping in rotational levels start influencing the excitation of the vibrational coherence and the Raman scattering processes. Therefore, once the dark state with rotational levels is formed, the excitation of vibrational coherence starts decreasing. It has been observed that the vibrational Raman transition saturates before the maximal coherence is reached because of the rotational Raman saturation [29].

Indeed, we have performed simulations for three- and four-level atoms. The results are shown in Fig. 4. For three-level atoms, the efficient excitation of vibrational coherence occurs as shown in Fig. 4(a). One can see excitation of the rotational coherence in Fig. 4(b). As seen in Fig. 4(c) for the four-level atoms, the excitation of rotational coherence prevents the excitation of vibrational coherence. Similar behavior can be observed for more sophisticated effects such as stimulated Raman adiabatic process (STIRAP) [36–38], where by adjusting properly the pulse shapes we demonstrate

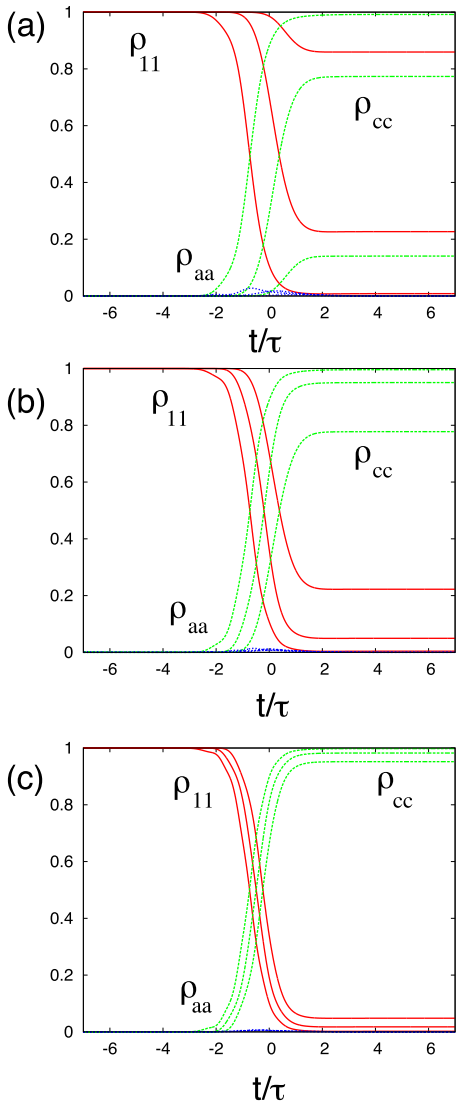

FIG. 9. Adiabatic passage population transfer in the λ system for different space positions inside the cell achieved with initial STIRAP pulses given by Eqs. (27) and (28). Their amplitudes are (a) $\Omega_{10,20} = 5\tau^{-1}$, (b) $\Omega_{10,20} = 7\tau^{-1}$, and (c) $\Omega_{10,20} = 10\tau^{-1}$. The ρ_{11} corresponds to population of level b_1.

very efficient population transfer from the ground state to the excited vibrational state. The time behavior of STIRAP laser pulses are shown in Fig. 5. The Gaussian pulses Ω_1 and Ω_2 are given by

$$\Omega_1(t) = \Omega_{10} \exp\left[-\frac{t^2}{2\tau^2}\right], \tag{27}$$

$$\Omega_2(t) = \Omega_{20} \exp\left[-\frac{(t-\tau_d)^2}{2\tau^2}\right], \tag{28}$$

where τ_d is the relative delay time between the laser pulses that have time duration τ, and Ω_{10} and Ω_{20} are the complex amplitude of the Gaussian pulses. We can see that for these pulses the population is transferred to close to 100% efficiency as shown in Fig. 6. For the case of the four-level model, the transferred population depends on the relation between the Rabi frequencies of the driving field and the splitting of the

ground level. The Gaussian pulses corresponding to the split ground states are

$$\Omega_{11}(t) = \Omega_{110} \exp\left[-\frac{t^2}{2\tau^2}\right], \tag{29}$$

$$\Omega_{12}(t) = \Omega_{120} \exp\left[-\frac{t^2}{2\tau^2}\right], \tag{30}$$

where Ω_{110} and Ω_{120} are the complex amplitude. In Fig. 7, one can see that with increasing laser fields, the STIRAP process of the adiabatic population transfer is strongly modified.

The population transfer depends on the ratio Δ/Ω_{120}, and for the fields with the Rabi frequency less than the rotational splitting ($\Omega_{120} < \Delta$), the efficiency is maximal as shown in Fig. 8(a). The comparative evolution of the vibrational and rotational coherences are shown in Fig. 8(b).

IV. PROPAGATION EFFECTS FOR STIRAP PULSES

Now we turn to propagation effects. The spatial and temporal evolution of Ω_1 and Ω_2 are given by

$$\left(c\frac{\partial}{\partial z} + \frac{\partial}{\partial t}\right)\Omega_1 = -i\Omega_{a1}^2 ab^*, \tag{31}$$

$$\left(c\frac{\partial}{\partial z} + \frac{\partial}{\partial t}\right)\Omega_2 = -i\Omega_{a2}^2 ac^*, \tag{32}$$

where the $\Omega_{a1,2}^2 = c\eta_{1,2}$ are the so-called cooperative frequencies. Using the basis of the "dark" and "bright" states, we can obtain the propagation equation for the effective Rabi frequency Ω_e as

$$\left(c\frac{\partial}{\partial z} + \frac{\partial}{\partial t}\right)\Omega_e = -i\Omega_a^2 aB^*. \tag{33}$$

Let us note that, for the adiabatic optical pulses, the population is in the dark state, $|D|^2 \simeq 1$, thus $aB^* \simeq 0$, and the effective Rabi frequency does not change during propagation such that $\Omega_e \simeq$ const. Finally, we obtain

$$\left(c\frac{\partial}{\partial z} + \frac{\partial}{\partial t}\right)\left(\frac{|\Omega_1|^2}{\Omega_{1a}^2} + \frac{|\Omega_2|^2}{\Omega_{2a}^2}\right) + \frac{\partial}{\partial t}|a|^2 = 0. \tag{34}$$

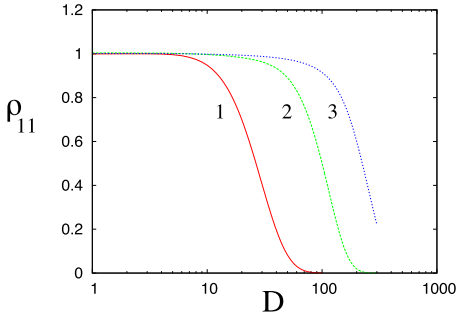

FIG. 10. Evolution of the STIRAP pulses for different space positions inside the cell filled with a three-level molecules achieved with initial STIRAP pulses given by Eqs. (27) and (28). The initial amplitudes of optical pulses are (a) $\Omega_{10,20} = 5\tau^{-1}$, (b) $\Omega_{10,20} = 7\tau^{-1}$, and (c) $\Omega_{10,20} = 10\tau^{-1}$.

It has a simple physical meaning and can be rewritten in the form of

$$\left(c\frac{\partial}{\partial z} + \frac{\partial}{\partial t}\right)(\mathcal{N}_1 + \mathcal{N}_2) + N\frac{\partial}{\partial t}|a|^2 = 0, \tag{35}$$

where $\mathcal{N}_1 = \frac{|E_1|^2}{4\pi\hbar\omega_1}$ and $\mathcal{N}_2 = \frac{|E_2|^2}{4\pi\hbar\omega_2}$ are the photon density of the laser beams and N is the molecular density. Equation (35) can be interpreted as the conservation of the photon flux and the population in the excited atomic state.

It is important for applications to study the effect of STIRAP along the laser pulses propagating through the media. We perform simulations, and the results of simulations are shown in Figures 9, 10, and 12. As expected, the laser pulses experience strong changes during propagation through the resonant media as shown in Fig. 10. Nevertheless, one can also see that the efficient Rabi frequency Ω_e does not practically change during propagation as it follows from Eq. (33) for adiabatic optical pulses.

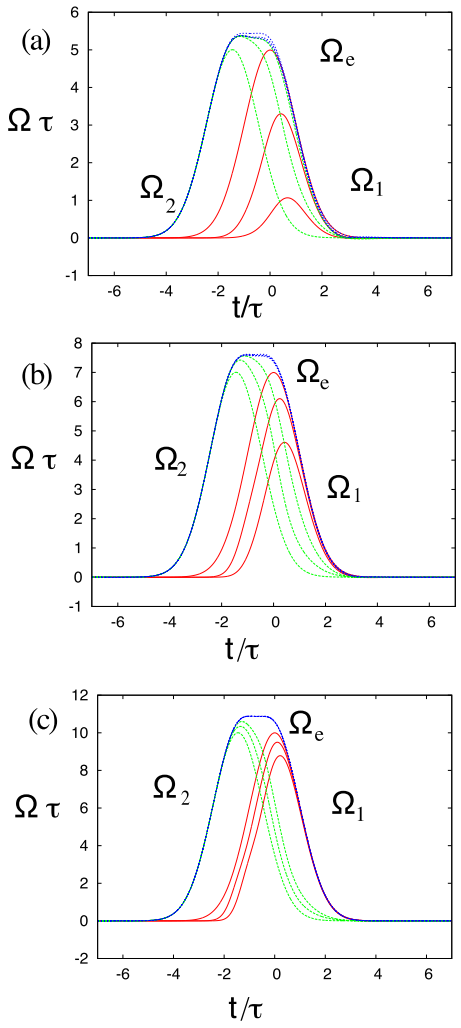

FIG. 11. Adiabatic passage population transfer achieved with STIRAP pulses as a function of optical density with different initial Rabi frequencies: (a) $\Omega_{10,20} = 5\tau^{-1}$, (b) $\Omega_{10,20} = 7\tau^{-1}$, and (c) $\Omega_{10,20} = 10\tau^{-1}$.

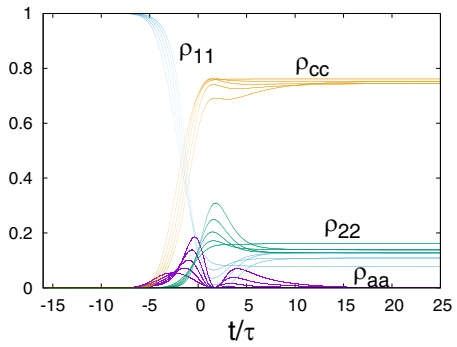

FIG. 12. The propagation of population transfer in a dense medium of four-level quantum system is shown for different space positions inside the cell achieved with initial STIRAP pulses given by Eqs. (27) and (28) and $\Omega_{10,20} = 7\tau^{-1}$.

Surprisingly, even with this strong change of laser pulses via propagation, we have demonstrated in our simulations that the effects of STIRAP are very prominent. The populations of ground levels are transferred very efficiently between vibrational levels as shown in Fig. 11. As an extension, the population transfer in a four-level system in an optically dense medium shows coherence pattern as expected during propagation (see Fig. 12). It is interesting to compare the energies of the laser pulses changes during propagation. The relative pulse energies can be characterized by

$$\mathcal{E}_{1,2} = \frac{\int_{-\infty}^{\infty} |\Omega_{1,2}(t,z)|^2 dt}{\int_{-\infty}^{\infty} |\Omega_{1,2}(t,z=0)|^2 dt}. \tag{36}$$

The dependence of relative change of pulse energies are shown in Fig. 13.

V. DISCUSSION AND CONCLUSIONS

In this paper, we have considered simple models containing three- or four-level molecules in the Λ configuration (see Fig. 2). The optical pulses are in two-photon resonance with the ground state and the vibrational state to provide excitation for Raman scattering, and the splitting of the ground-state

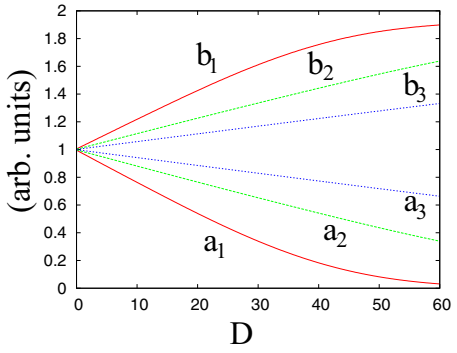

FIG. 13. Dependence of the energies of pulses propagating through the media with different initial Rabi frequencies. Adiabatic passage population transfer achieved with STIRAP pulses with initial Rabi frequencies: (a) $\Omega_{10,20} = 5\tau^{-1}$, (b) $\Omega_{10,20} = 7\tau^{-1}$, and (c) $\Omega_{10,20} = 10\tau^{-1}$,

simulates rotational levels. Because of the dark state formation, the modification of Raman coherence occurs and the dark state has strong influence on the STIRAP. We have also studied STIRAP in the extended media, taking into account the propagation of optical pulses. The importance of these effects are related to modification of the Raman spectroscopy due to molecular rotational motion.

On the other hand, the effects reported here are related to the presence of additional levels such as the magnetic sublevels for alkali metal vapors. Indeed, the Rb vapor demonstrates many coherent effects, in particular, the coherent Raman scattering enhancement via maximal coherence in atoms [39] that demonstrating the importance of quantum coherence. The efficiency of the STIRAP to the helium Rydberg state ($2\,^3S \rightarrow 3\,^3P \rightarrow$ nL, $n = 24$) was thoroughly studied in Ref. [40], where some deviation from the simplified theory has been reported. Our approach suggests another reason for lower efficiency originated from the effects of the magnetic sublevels.

The femtosecond coherent anti-Stokes Raman spectroscopy has been used extensively in time-resolved nonlinear spectroscopy research [9]. The results reported in this paper demonstrate new physics when femtosecond ultrafast laser pulses are used for Raman excitation and Raman spectroscopy. For example, the femtosecond ultrafast laser pulses with broad spectra may overlap with rotational levels of molecular system, and the resultant interaction subsequently forms coherently populated states. The configuration of trapped states involving rotational energy levels will interfere with pure Raman excitation of vibrational coherences, crucial to contemporary spectroscopies of molecular identification, etc.

We have studied the role of the rotational levels not only on the electromagnetically induced transparency and on the coherent population trapping but also on the fractional STIRAP that allows researchers to obtain the maximal coherence. Even though for the fractional STIRAP optical pulses we have seen strong modification of the population transfer between the molecular levels similar to the STIRAP, we have found that the excitation of the vibrational coherence by fractional STIRAP pulses turns out to have less influence on the presence of the rotational levels.

We have been using the parameters for relaxation rates in the molecular and atomic systems from experimental works [17,20,23]. We study the propagation of optical beams and demonstrate that the population transfer is very robust with respect to propagation in the dense media. The propagation is influenced by the molecular rotational structure, but nevertheless it stays robust. The simulated plot in Fig. 12 shows the population transfer tendency as the applied pulse propagates through the medium. Optical field intensity affects the population transfer such that the stronger field demonstrates a strong coherence, influencing better population transfer in a three-level system. The deviation from perfect adiabatic transfer is far more symmetrical (linear systems) and can be seen as a tool for selective population transfer for coherently prepared system. The fractional-STIRAP can be improved to estimate the precise thickness of the medium under controlled optical field excitation. With the propagation of the optical pulse, the system starts approaching a coherent superposition

of coupled states. This presents the maximal coherence of Raman transition for an extended media. It is interesting to note that even with expected laser pulse variation observed, the effective Rabi frequency does not vary during propagation. Applied field variation is shown in the form of Rabi frequency plotted against optical thickness of the medium. As expected, the strong coherence with the applied field retains its shape for longer optical depth.

It is interesting to compare laser pulses energy changes during propagation. The propagation of pulses and their efficiency to perform population transfer is essential to the applications involving an extended optically dense medium. The linear resonant absorption regime is well studied and improved over past decades, but the application involving the three- and four-level systems may explain the deviation observed in gaseous medium. For example, the efficiency of STIRAP for Rydberg states [41] performed in helium. Simple three-level models of STIRAP predict 100% excitation probability, but the raw measurements are typically around half of this and vary with both n and l of the Rydberg states selected for excitation. It is important that magnetic sublevels be taken into account because they can form the additional dark states that prevent a complete population transfer, as can occur in a simple three-level scheme.

The propagation of optical pulse in an optically dense medium shows a dependence on effective Rabi frequency. The physics of formation of dark states is strongly influenced by the presence of the fourth and more levels. For the case of a four-level scheme, we have shown explicitly the dark states that are formed under the action of the laser fields. This is very important for atomic and molecular media and for Raman and coherent Raman spectroscopy. It can also be important for the near-field interaction due to the strong electromagnetic field induced by resonant localized plasmons that can result in a strong coupling of excitonic states or formation of hybrid exciton-plasmon modes in quantum confined structures. Silver nanoislands nucleated on molybdenum disulfide (MoS_2) is an ideal platform for such interaction (see Ref. [42]).

ACKNOWLEDGMENTS

We thank Adam Voigt, Marshall Rogers, Konstantin Dorfman, and Stephen Schiller for fruitful discussions, comments, and suggestions. We also gratefully acknowledge the support from the Advanced Materials and Manufacturing Processes Institute at the University of North Texas seed research project.

APPENDIX

The state vector for the three-level atom with a rotational level structure is written as

$$|\psi\rangle = \sum_j (a_j|a_j\rangle + b_j|b_j\rangle + c_j|c_j\rangle). \tag{A1}$$

The Hamiltonian with changes to accommodate possible $J(J+1)$ interacting levels can be written as

$$H = \hbar \sum_{j,j'} \Omega_{1j}^* e^{i\Delta_{1j}t}|b_j\rangle\langle a_{j'}| + \Omega_{2j}^* e^{i\Delta_{j}t}|c_j\rangle\langle a_{j'}| + \text{adj.} \tag{A2}$$

Let us, for simplicity, restrict discussion to a single rotational split of a ground level in order to analyze the interaction. Thus, we consider a four-level molecular medium interacting with the probe and coupling fields. For angular frequencies ω_{ab_1} and ω_{ab_2} corresponding to the allowed transitions $|a\rangle \rightarrow |b_1\rangle$ and $|a\rangle \rightarrow |b_2\rangle$, the interaction Hamiltonian in the rotating-wave approximation can be written as

$$H = \hbar[\Omega_{11}^* e^{i\Delta_{11}t}|b_1\rangle\langle a| + \Omega_{12}^* e^{i\Delta_{12}t}|b_2\rangle\langle a| \tag{A3}$$

$$+\Omega_2^* e^{i\Delta_2 t}|c\rangle\langle a| + ,.]. \tag{A4}$$

Here $\Omega_{11} = \wp_{ab_1}E_1/\hbar$ and $\Omega_{12} = \wp_{ab_2}E_1/\hbar$ are the coupling Rabi frequencies, $\Delta_{11} = \omega_{ab_1} - \omega_1$ and $\Delta_{12} = \omega_{ab_2} - \omega_1$ are the detunings for probe laser beam, and $\wp_{ab_1}$ and $\wp_{ab_2}$ are the corresponding dipole momenta of the transitions. The state vector for the four-level system is written as

$$|\psi\rangle = a|a\rangle + b_1|b_1\rangle + b_2|b_2\rangle + c|c\rangle. \tag{A5}$$

[1] R. W. Boyd, *Nonlinear Optics* (Academic Press, Boston, 1992).

[2] Y. R. Shen, *The Principles of Nonlinear Optics* (Wiley, New York, 1984).

[3] B. Schrader (Ed.), *Infrared and Raman Spectroscopy* (VCH, Tokyo, 1995).

[4] M. O. Scully, G. W. Kattawar, B. P. Lucht, T. Opatrny, H. Pilloff, A. Rebane, A. V. Sokolov, M. S. Zubairy, FAST CARS: Engineering a laser spectroscopic technique for rapid identification of bacterial spores, PNAS **99**, 10994 (2002).

[5] D. Pestov, M. C. Zhi, Z.-E. Sariyanni, N. K. Kalugin, A. A. Kolomenskii, R. Murawski, G. G. Paulus, V. A. Sautenkov, H. Schuessler, A. V. Sokolov, G. R. Welch, Y. V. Rostovtsev, T. Siebert, D. A. Akimov, S. Graefe, W. Kiefer, M. O. Scully, Visible and UV coherent Raman spectroscopy of dipicolinic acid, PNAS **102**, 14976 (2005).

[6] D. Pestov, R. K. Murawski, G. O. Ariunbold, Xi Wang, M. Zhi, A. V. Sokolov, V. A. Sautenkov, Y. V. Rostovtsev, A. Dogariu, Y. Huang, and M. O. Scully, Optimizing the laser pulse configuration for coherent Raman spectroscopy, Science **316**, 265 (2007).

[7] F.-K. Lu, M. Ji, D. Fu, X. Ni, C. W. Freudiger, G. Holtom, and X. S. Xie, Multicolor stimulated Raman scattering microscopy, Mol. Phys. **110**, 1927 (2012).

[8] D. Fu, G. Holtom, C. W. Freudiger, X. Zhang, and X. S. Xie, Hyperspectral imaging with stimulated Raman scattering by chirped femtosecond lasers, J. Phys. Chem. B **117**, 4634 (2013).

[9] S. Roy, J. R. Gord, and A. K. Patnail, Recent advances in coherent anti-Stokes Raman scattering spectroscopy: Fundamental developments and applications in reacting flows, Prog. Energy Combust. Sci. **36**, 280 (2010).

[10] E. Arimondo, Coherent population trapping in laser spectroscopy, in *Progress in Optics*, edited by E. Wolf (Elsevier Science, Amsterdam, 1996), Vol. XXXV, p. 257.

[11] M. O. Scully and M. S. Zubairy, *Quantum Optics* (Cambridge University Press, Cambridge, UK, 1997).

[12] S. E. Harris, Electromagnetically induced transparency, Phys. Today **50**(7), 36 (1997).

[13] S. E. Harris, Electromagnetically Induced Transparency with Matched Pulses, Phys. Rev. Lett. **70**, 552 (1993).

[14] M. Fleischhauer, A. Imamoglu, and J. P. Marangos, Electromagnetically induced transparency: Optics in coherent media, Rev. Mod. Phys. **77**, 633 (2005).

[15] O. Kocharovskaya, and Ya. I. Khanin, Population trapping and coherent bleaching of a three-level medium by a periodic train of ultrashort pulses, Zh. Eksp. Teor. Fiz. **90**, 1610 (1986) [Sov. Phys. JETP **63**, 945 (1986)].

[16] V. A. Sautenkov, Y. V. Rostovtsev, C. Y. Ye, G. R. Welch, O. Kocharovskaya, and M. O. Scully, Electromagnetically induced transparency in rubidium vapor prepared by a comb of short optical pulses, Phys. Rev. A **71**, 063804 (2005).

[17] V. A. Sautenkov, H. Li, Y. V. Rostovtsev, and M. O. Scully, Ultradispersive adaptive prism based on a coherently prepared atomic medium, Phys. Rev. A **81**, 063824 (2010).

[18] F. Abeles, *Optical Properties of Solids* (North-Holland, Amsterdam, 1972).

[19] L. V. Hau, S. E. Harris, Z. Dutton, and C. H. Behroozi, Light speed reduction to 17 metres per second in an ultracold atomic gas, Nature (London) **397**, 594 (1999); C. Liu, Z. Dutton, C. H. Behroozi, and L. V. Hau, Observation of coherent optical information storage in an atomic medium using halted light pulses, *ibid.* **409**, 490 (2001).

[20] M. M. Kash, V. A. Sautenkov, A. S. Zibrov, L. Hollberg, G. R. Welch, M. D. Lukin, Y. Rostovtsev, E. S. Fry, and M. O. Scully, Ultraslow Group Velocity and Enhanced Nonlinear Optical Effects in a Coherently Driven Hot Atomic Gas, Phys. Rev. Lett. **82**, 5229 (1999); D. Budker, D. F. Kimball, S. M. Rochester, and V. V. Yashchuk, Nonlinear Magneto-optics and Reduced Group Velocity of Light in Atomic Vapor with Slow Ground State Relaxation, *ibid.* **83**, 1767 (1999).

[21] L. J. Wang, A. Kuzmich, and A. Dogariu, Gain-assisted superluminal light propagation, Nature (London) **406**, 277 (2000); A. Dogariu, A. Kuzmich, and L. J. Wang, Transparent anomalous dispersion and superluminal light-pulse propagation at a negative group velocity, Phys. Rev. A **63**, 053806 (2001).

[22] G. S. Agarwal, T. N. Dey, and S. Menon, Knob for changing light propagation from subluminal to superluminal, Phys. Rev. A **64**, 053809 (2001).

[23] E. E. Mikhailov, V. A. Sautenkov, Y. V. Rostovtsev, and G. R. Welch, Absorption resonance and large negative delay in rubidium vapor with a buffer gas, J. Opt. Soc. Am. B **21**, 425 (2004); Q. Sun, Y. V. Rostovtsev, J. P. Dowling, M. O. Scully, and M. S. Zubairy, Optically controlled delays for broadband pulses, Phys. Rev. A **72**, 031802(R) (2005).

[24] A. B. Matsko, Y. V. Rostovtsev, M. Fleischhauer, and M. O. Scully, Anomalous Stimulated Brillouin Scattering via Ultraslow Light, Phys. Rev. Lett. **86**, 2006 (2001).

[25] Y. V. Rostovtsev, Z.-E. Sariyanni, and M. O. Scully, Electromagnetically Induced Coherent Backscattering, Phys. Rev. Lett. **97**, 113001 (2006).

[26] L. Allen and J. H. Eberly, *Optical Resonance and Two Level Atoms* (Dover, New York, 1987).

[27] D. Sun, Z.-E. Sariyanni, S. Das, and Y. V. Rostovtsev, Propagation of 0π pulses in a gas of three-level atoms, Phys. Rev. A **83**, 063815 (2011).

[28] Z.-E. Sariyanni, D. Sun, and Y. V. Rostovtsev, Stimulated Raman spectroscopy with 0π pulses, Opt. Lett. **39**, 766 (2014).

[29] A. K. Patnaik, S. Roy, and J. R. Gord, Saturation of vibrational coherent anti-Stokes Raman scattering mediated by saturation of the rotational Raman transition, Phys. Rev. A **87**, 043801 (2013).

[30] A. K. Patnaik, S. Roy, and J. R. Gord, Ultrafast saturation of resonant optical processes, Phys. Rev. A **90**, 063813 (2014).

[31] A. K. Patnaik, S. Roy, and J. R. Gord, Lineshape dependence of ultrafast saturation of absorption and fluorescence, Phys. Scr. T **T165**, 014031 (2015).

[32] A. K. Patnaik, S. Roy, and J. R. Gord, Ultrafast saturation of electronic-resonance-enhanced coherent anti-Stokes Raman scattering and comparison for pulse durations in the nanosecond to femtosecond regime, Phys. Rev. A **93**, 023812 (2016).

[33] P. J. Wrzesinski, H. U. Stauffer, J. B. Schmidt, S. Roy, and J. R. Gord, Single-shot thermometry and OH detection via femtosecond fully resonant electronically enhanced CARS (FREE-CARS), Opt. Lett. **41**, 2021 (2016).

[34] H. U. Stauffer, S. Roy, J. B. Schmidt, P. J. Wrzesinski, and J. R. Gord, Two-color vibrational, femtosecond, fully resonant electronically enhanced CARS (FREE-CARS) of gas-phase nitric oxide, J. Chem. Phys. **145**, 124308 (2016).

[35] Y. Rostovtsev, I. Protsenko, H. Lee, and A. Javan, From laser-induced line narrowing to electromagnetically induced transparency in a Doppler-broadened system, J. Mod. Opt. **49**, 2501 (2002); H. Lee, Y. Rostovtsev, C. J. Bednar, and A. Javan, From laser-induced line narrowing to electromagnetically induced transparency: Closed system analysis, Appl. Phys. B **76**, 33 (2003).

[36] N. V. Vitanov, A. A. Rangelov, B. W. Shore, and K. Bergmann, Stimulated Raman adiabatic passage in physics, chemistry, and beyond, Rev. Mod. Phys. **89**, 015006 (2017).

[37] N. V. Vitanov, M. Fleischhauer, B. W. Shore, and K. Bergmann, Coherent manipulation of atoms molecules by sequential laser pulses, Adv. At., Mol., Opt. Phys. **46**, 55 (2001).

[38] R. Netz, A. Nazarkin, and R. Sauerbrey, Observation of Selectivity of Coherent Population Transfer Induced by Optical Interference, Phys. Rev. Lett. **90**, 063001 (2003).

[39] V. A. Sautenkov, C. Y. Ye, Y. V. Rostovtsev, G. R. Welch, and M. O. Scully, Enhancement of field generation via maximal atomic coherence prepared by fast adiabatic passage in Rb vapor, Phys. Rev. A **70**, 033406 (2004).

[40] D. Yuan, STIRAP on helium: Excitation to Rydberg states, Ph.D. thesis, State University of New York at Stony Brook, Stony Brook, NY, 2015, http://graduate.physics.sunysb.edu/announ/theses/sun-yuan-december-2013.pdf.

[41] X. Lu, Excitation of helium to Rydberg states using STIRAP, Ph.D. thesis, State University of New York at Stony Brook, Stony Brook, NY, 2011.

[42] Y. Poudel, G. N. Lim, M. Moazzezi, Z. Hennighausen, Y. Rostovtsev, F. DSouza, S. Kar, and A. Neogi, Active control of coherent dynamics in hybrid plasmonic MoS_2 monolayers with dressed phonons, arXiv:1810.02056.